Submitted to: *Main Group Chemistry*

Effect of carbon nanotubes on calcium carbonate/calcium silicate phase and morphology

Virginia Gomez,[a] Covadonga Correas,[a] and Andrew R. Barron[a,b,c]*

[a] *Energy Safety Research Institute (ESRI), College of Engineering, Swansea University, Bay Campus, Swansea, SA1 8EN, Wales, UK*

[b] *Department of Chemistry, Rice University, Houston, Texas 77005, USA*

[c] *Department of Materials Science and Nanoengineering, Rice University, Houston, Texas 77005, USA*

Abstract

The composition and microstructure of different $CaCO_3$-Ca_2SiO_4-carbon nanotube composites have been studied. Materials have been characterized by X-ray diffraction (XRD), high resolution scanning electron microscopy (SEM), thermogravimetric/differential thermal analysis (TG/DTA), and Fourier-transform infrared (FTIR) spectroscopy. The morphology and structure of the inorganic systems are affected by the presence of multiwall carbon nanotubes (MWCNT) during the hydration processes and the nature of the MWCNT/SDS interface plays a role in the curing stages of the composite enhancing the growth of calcium silicate.

Keywords: Calcium; carbonate; carbon nanotubes, silicate; microstructure, hydration.

* Corresponding author. Tel.: +44-(0)1792-606930; E-mail: a.r.barron@swansea.ac.uk, arb@rice.edu.

1. Introduction

Carbon nanotubes (CNTs) have been investigated as additives for a range of nano-composites [1-4] due to their high Young's modulus [5,6]. Several cement-based composite materials have included CNTs in their composition [7-9], since the combination of these materials offers great functional advantages over materials now employed in construction [10]. The majority of research has concentrated on the inclusion of CNTs during traditional composite processing [11,12]; however, there has been a recent interest in what the effect the presence of CNTs [13,14]. A recent work reports on the effects of carbon nanotubes (CNTs) on the microstructure and properties of carbon fiber-reinforced silicon carbide (C/SiC) composites [15]. We have reported that the synthesis of composites of $CaCO_3$ with fullerenes and single walled carbon nanotubes (SWCNTs) results in amorphous phases with unique and interesting morphologies [16]. These results suggested that the interface between the carbon nanomaterial and the growth medium is important, and the following work done by our group confirmed that the identity of functionalization (covalent versus non-covalent) was indeed important for $CaCO_3$ growth [17]. In further work we observed that with Portland cement showed that the CNTs accelerate the hydration reaction of the tricalcium silicate ($3CaO.SiO_2$ or C3S) and the morphology of both the tricalcium aluminate ($3CaO.Al_2O_3$ or C3A) and C3S hydration products were affected by the SWCNTs [18]. The effectiveness of the different dispersants on the microstructure and properties of CNTs alumina composites have been studied [19]. We have reported that surfactants typically used to solubilize CNTs also modify the morphology in the $CaCO_3/SiO_2$ system [20] and so it is important to differentiate between the effects of the CNTs and those of the surfactant. The hydration of the calcium silicate materials reported by Allen *et al.* determines the final morphology and particle size, which is related with various mechanical and chemical properties of cement based materials as well as other composites [21], so a study of the effect of the CNTs on the hydration processes in different $CaCO_3/SiO_2$ systems is of interest given the effects observed in the SiO_2 and $CaCO_3$ systems [16,22,23].

In the current work, we aimed to complete the reaction matrix of $CaCO_3$ + CNTs [13], $CaCO_3$ + silica source + surfactant [20], and silica + surfactant [24]. Composite materials

were synthesized using multi-walled carbon nanotubes (MWCNTs) as additives to inorganic $CaCO_3/SiO_2$ matrices, using fumed silica (FS) or silicic acid (SA) as the silica source, to determine the effects of the sodium dodecyl sulfate (SDS) surfacted MWCNT in the growth, crystallization and morphology. In addition, the effect of MWCNT/SDS on the hydration of pre-formed commercial calcium silicate ($CaSiO_3$) was investigated.

2. Experimental section

2.1. Materials and methods

Calcium carbonate, fumed silica (FS), silicic acid (SA) and commercial $CaO\text{-}SiO_2$ (c-$CaO\text{-}SiO_2$) were purchased from Sigma Aldrich (ACS grade) and used as supplied. Multiwall carbon nanotubes (MWCNTs) were prepared using a tabletop horizontal tube reactor (Nanotech Innovations SSP-354) as previously reported [25] and were used after acid purification [26], see Fig. 1.

[Insert Fig. 1 here]

Samples were characterized by scanning electron microscopy (SEM) using an Ultra-High Resolution FE-SEM S-4800 coupled with an energy dispersive X-ray analyzer (Inca X-ray analysis system, Oxford Instruments, Abingdon, United Kingdom) used for the EDX analysis. The crystallographic structure of the products was determined by XRD using a Bruker AXS D8 Advance diffractometer (Cu-K_α, λ = 1.5418 Å) with an LINXEYE detector between 10° and 70° (2θ), with 2θ increments of 0.02° and counting time of 0.5 s. Differential thermal/thermogravimetric analysis (DT/TGA) of the samples were performed on a TA Q600 instrument. The samples were heated under flowing air (100 mL/min) from room temperature to 1300 °C with a heating rate of 20 °C/min. The exhaust gas from the TGA was monitored using a heated sample transfer line (350 °C) and a Thermoscientific i510 FTIR. Scans were taken approximately every 36 seconds for the duration of the heating cycle. This FTIR equipment was also used to carry out IR analysis of all the samples, recording spectra in the 650-4000 cm^{-1} region with 16 scans.

2.2. Sample preparation

In a typical experiment, $CaCO_3$ (200 mg) was added to distilled water (250 mL) and stirred at ambient pressure under a flow of CO_2 for 1 hour. H_4SiO_4 (20 mg) were added, whilst stirring and the CO_2 bubbling for 4 hours [20]. The reaction mixture was then stirred under a CO_2 atmosphere for a further 20 hours. Finally, the sample was filtered by gravity and dried in an oven at 70 °C for 1 hour and characterized before the curing process. The reactant powders were mixed following the amounts indicated in Table 1. In order to ensure a homogeneous mixing, MWCNTs were dispersed in a 1% aqueous solution of sodium dodecyl sulfate (SDS) over 30 min in an ultrasonic bath to form 1 mg/mL dispersion. The corresponding amount of MWCNTs dispersion or SDS solution was added to the reactants mixture and placed in an ultrasonic bath for 5 min. The mixture was aged for one or two weeks under ambient indoor conditions (~20 °C, 1 atm). Finally, all samples were dried in an oven at 70 °C for 1 hour.

[Insert Table 1 here]

3. Results and discussion

Table 1 summarizes the reactions employed for the different samples for different $CaCO_3/SiO_2$ combinations using multiwall carbon nanotubes (MWCNTs) as an additive material.

3.1. Effect of MWCNTs on the $CaCO_3$/fumed silica system

Fig. 2 shows the SEM micrographs of sample **2** prepared from the reaction of $CaCO_3$ and fumed silica (FS) in the presence of SDS surfacted MWCNTs (Fig. 2a and b), in comparison with that of sample **1** prepared without the MWCNTs (Fig. 2c). As was reported previously [18], the presence of the surfactant SDS results in the formation of a textured particulate structure containing a fraction of almost spherical particles. The presence of residual SDS is confirmed from the presence of sodium and sulfur in the EDX spectrum (Fig. 2d). The sample prepared with the MWCNTs shows no spherical particles, but a sheet-like structure (Fig. 2a),

while the insertion of MWCNTs (arrows) between the hydration products can be seen in Fig. 2b. Similar results have been observed in the cement based composites literature [7].

[Insert Fig. 2 here]

The XRD for sample **2** after curing for 1 week (Fig. 3a) shows in addition to peaks associated with crystalline calcite ($CaCO_3$) two broad peaks. The peak at 20° is associated with silica [27], while the peak centered close to 30° is be attributed to highly polycrystalline Ca_2SiO_4 [28] based upon changes that occur upon sintering (see below). The spectrum of sample **2** (in the presence of MWCNTs) is similar, although the relative intensity of this latter amorphous phase is higher, suggesting that the MWCNT favour the growth of this phase.

FTIR of samples **1** and **2** (Fig. 4a) confirms the presence of calcite, as the main asymmetric band (ν_3) and symmetric vibration (ν_4) of CO_3 at 1391 and 711 cm^{-1} are characteristic of crystalline calcium carbonate phases [29,30]. A broad band, centered at 1083 cm^{-1}, appears in the spectrum of the sample without MWCNT and is associated to silica in the presence of a modifier oxide, such as calcium compounds [31]. This band is significantly diminished in the spectrum of the sample with MWCNT (sample **2**) indicating that the amount of silica is lower, probably due to Ca_2SiO_4 (C2S) formation. The remaining bands (1795, 1390, 1085 and 870 cm^{-1}) represent the vibrations of the carbonate ions, except a 1217 cm^{-1} peak, corresponding to the skeletal vibration of the bridge S-O stretch in the SDS molecule [32].

[Insert Fig. 4 here]

3.2. Effect of MWCNTs on the $CaCO_3$/silicic acid system

The SEM micrographs of samples **3** and **4** after curing for 1 week are shown in Fig. 5. As has been reported [20] the addition of SDS to a $CaCO_3$/silicic acid (SA) reaction results in the formation of large (20 μm) crystallites (of calcite, see below) in a matrix of smaller particles of less well defined shapes (Fig. 5a and b). In dramatic contrast, the presence of the

MWCNTs results in a ribbon morphology, several microns in length and hundreds of nanometres wide (Fig. 5c and d). This latter observation is reminiscent of silica coated CNTs [22,23], which is expected since SA was used to grow silica coatings on SDS-solubilized SWCNTs. Thus, it would appear that the initial formation of SiO_2-coated MWCNTs is followed by silicate growth on the template, while excess $CaCO_3$ crystals may be seen as large crystallites (ca. 10 μm).

[Insert Fig. 5 here]

The XRD of samples **3** and **4** follow the trends observed for samples **1** and **2**, i.e., the presence of the MWCNTs appears to enhance the formation of Ca_2SiO_4 (C2S) see Fig. 3b. The FTIR spectra show the calcite bands (see above) together with the SDS bands, which are more intense in the case of the sample with MWCNT. The peaks at 2956, 2917, 2850 and 1467 cm^{-1} corresponding to CH_2 stretching and bending modes which is characteristic of a polar environment, the 1216 cm^{-1} peak corresponding to skeletal vibration involving the bridge S–O stretch, the 995 cm^{-1} peak corresponding to C–C band stretching and 832 cm^{-1} peaks corresponding to asymmetric C–H bending of the CH_2 group [32]. In this case, in sample **4** (with the MWCNTs) apart from the 1081 cm^{-1} band, corresponding to silica in presence of Ca^{2+}, it is possible to observe a group of bands around 1050 cm^{-1}, which have been associated to silicate modes in other works [31].

3.3. Effect of MWCNTs on the hydration of preformed $CaCO_3$-SiO_2

A commercial sample of CaO-SiO_2 was hydrated for one week in the presence of SDS (sample **5**) or SDS-MWCNT (sample **6**). In the presence of SDS the hydration of CaO-SiO_2 appears similar to prior to hydration, and consists of a particulate structure. In contrast, the presence of MWCNTs results in the formation of a small number of smooth platelet regions. The identity of these features appears to be associated with the formation of Ca_2SiO_4 (C2S), since sintering both samples to 1300 °C (Fig. 6b and d) results in an increase in these regions for both samples and coincides with C2S crystallization.

[Insert Fig. 6 here]

XRD patterns of these samples after the curing clearly showed the promoting effect of the MWCNT in the Ca_2SiO_4 growth (Fig. 3c), even if the broadness of the peaks suggest a poorly crystalline (i.e., very small crystal domains) sample. Sintering the CaO-SiO_2 sample to 1300 °C results in the formation of crystalline Ca_2SiO_4 larnite (JCPDS 33-0302) along with SiO_2 cristobalite (JCPDS 101-0938) and $CaSiO_3$ pseudowollastonite (JCPDS 900-2250). Interestingly, the presence of MWCNTs appear to inhibit significant crystallization of the Ca_2SiO_4.The FTIR spectrum of samples **5** and **6** show the broad band at 1000-1300 cm^{-1} associated with the stretching vibration of Si-O-Si.

In order to probe the Ca_2SiO_4 formation, a DT/TGA has been carried out on samples **5** and **6**. From Fig. 7 it can be seen that at around 100 °C, the external water is lost in both samples occurs, with a comparable mass loss (ca. 6%). At around 250 °C, an exothermic transition with the 10-12% mass loss is due to the decomposition of the SDS and the dehydration of calcium silicate hydrates, in both samples, while the exothermic transition in sample **6** above 600 °C, corresponding to the MWCNT decomposition [34,35]. In the absence of MWCNTs (sample **5**) there is a distinct endotherm at 920 °C associated with the crystallization of Ca_2SiO_4.

The same endotherm is only marginally above the baseline in sample **6**, consistent with the XRD results that indicate significantly lower crystalline Ca_2SiO_4 after thermolysis (Fig. 3c). In the case of CaO-SiO_2/SDS (sample **5**) there is a 2-stage exothermic decomposition (1000 and 1100 °C) in which the second step shows a significantly larger exothermic peak in the DTA. A 2-stage mass loss is also observed for sample **6**; however, the 2^{nd} steps temperature is significantly lowered (1080 °C). This difference may be due to the Ca:Si ratio since this transition temperature increases with the increased Ca:Si ratio [37].

[Insert Fig. 7 here]

4. Conclusions

The results of the present study suggest that the presence of the anionic surfactant SDS coupled with the carbon nanotubes have a clear effect on the growth of hydrated silicates. SDS-surfacted MWCNTs acts as a template for growing silicates and alters the amount of certain phases present in the samples. For the hydration of $CaSiO_3$ there is an enhancement in Ca_2SiO_4 (C2S) formation, albeit poorly crystalline in nature, while the presence of MWCNTs also appears to inhibit crystallization upon thermolysis. For the reaction of $CaCO_3$ with fumed silica or silicic acid there is a small change in the formation of poorly crystalline (amorphous) Ca_2SiO_4, and for fumed silica (FS) there is only a small change in morphology. However, with silicic acid (SA) the morphology is dominated by the formation of ribbon-like particles template by the MWCNTs. This process is most probably related to the known complexation of Ca^{2+} to the negatively charged SDS polar groups [38], and the importance of the surfactant modified interfacial interaction in CNT composites [39,40].

Acknowledgments

Financial support was provided by the Welsh Government Sêr Cymru Programme, the Robert A. Welch Foundation (C-0002), and through FLEXIS, which is part-funded by the European Regional Development Fund (ERDF), through the Welsh Government. The authors thank Dr. Cecile Charbonneau (SPECIFIC, Swansea University) for the use of the XRD equipment.

References

[1] D. S. Jensen, S. S. Kanyal, V. Gupta, M. A. Vail, A. E. Dadson, M. Engelhard, R. Vanfleet, R. C. Davis, M. R. Linford, Stable microfabricated thin layer chromatography plates without volume distortion on patterned, carbon and Al_2O_3-primed carbon nanotube forests*, J. Chromatogr. A* 2012, *1257,* 195-203.

[2] L. Chen, L. Youji, X. Peng, L. Ming, Z. Mengxiong, Carbon nanotube embedded mesoporous titania pore-hole inorganic hybrid materials with high thermal stability, improved crystallinity and visible-light driven photocatalytic performance*, Micropor. Mesopor. Mat.* **195** (2014), 319-329.

[3] H. R. Jafry, R. C. Tailor, G. Ibbott, A. R. Barron, Coating carbon nanotubes with lead sulfide and bismuth siulfide, *Main Group. Chem.* **12** (2013), 67-86.

[4] A. Jitianu, T. Cacciaguerra, R. Benoit, S. Delpeux, F. Beguin, S. Bonnamy, Synthesis and characterization of carbon nanotubes–TiO_2 nanocomposites, *Carbon* 42 (2004), 1147-1151.

[5] J. P. Salvetat, G. A. Briggs, J. M. Bonard, R. R. Bacsa, A. J. Kulik, T. Stöckli, N. A. Burnham, L. Forró, Elastic and shear moduli of single-walled carbon nanotube ropes, *Phys. Rev. Lett.* **82** (1999), 944–947.

[6] Lupo, F., Kamalakaran, R., Scheu, C., Grobert, N., and Rühle, M., Microstructural investigations on zirconium oxide–carbon nanotube composites synthesized by hydrothermal crystallization, *Carbon* **42** (2004), 1995–1999.

[7] T. Nochaiya, A. Chaipanich, Behavior of multi-walled carbon nanotubes on the porosity and microstructure of cement-based materials, *Appl. Surf. Sci.* **257** (2011), 1941-1945.

[8] G. Y. Li, L. B. Zeng, L. Wang, B. Yan, J. Fan, A method to improve the microstructure and mechanical properties of carbon nanotube/cement matrix*, Gongneng Cailiao* **45** (2014), 18107-18111.

[9] B. Wang, Y. Zhang, H. Ma, Porosity and pore size distribution measurement of cement/carbon nanofiber composites by ^{1}H low field nuclear magnetic resonance, *J. Wuhan Univ. Technol., Mater. Sci. Ed.* **29** (2014), 82-88.

[10] J. Rieger, M. Kellermeier, L. Nicoleau, Formation of nanoparticles and nanostructures—an industrial perspective on $CaCO_3$, cement, and polymers, *Angew. Chem. Int. Ed.* **53** (2014), 12380-12396.

[11] A. Peigney, Ch. Laurent, E. Flahaut, A. Rousset, Carbon nanotubes in novel ceramic matrix composites, *Ceram. Int.* **26** (2000), 677–683.

[12] T. Kuzumaki, O. Ujiie, H. Ichinose, K. Ito, Mechanical characteristics and preparation of carbon nanotube fiber-reinforced Ti composite, *Adv. Eng. Mater.* **2** (2000), 416–418.

[13] L. J. Groven, J. A. Puszynski, Effect of carbon nanotube addition on morphology of SHS synthesized materials, *Int. J. Self-Propag. High-Temp. Synth.* **16** (2007), 189-198.

[14] L. A. Dobrzański, M. Macek, B. Tomiczek, Effect of carbon nanotubes content on morphology and properties of AlMg1SiCu matrix composite powders, *AMSE* **69** (2014), 12-18.

[15] H. Mei, H. Wang, N. Zhang, H. Ding, Y. Wang, Q. Bai, Carbon nanotubes introduced in different phases of C/PyC/SiC composites: Effect on microstructure and properties of the materials, *Compos. Sci. Technol.* **115** (2015), 28-33.

[16] R. E. Anderson, A. R. Barron, Effect of carbon nanomaterials on calcium carbonate crystallization, *Main Group Chem*. **4** (2005), 279-289.

[17] D. Tasis, S. Pispas, C. Galiotis, N. Bouropoulos, Growth of calcium carbonate on non-covalently modified carbon nanotubes, *Mater. Lett.* 61 (2007), 5044-5046.

[18] J. Makar, G. W. Chan, Growth of cement hydration products on single-walled carbon nanotubes, *J. Am. Ceram. Soc.* **92** (2009), 1303-1310.

[19] F. Inam, A. Heaton, P. Brown, T. Peijs, M. J. Reece, Effects of dispersion surfactants on the properties of ceramic–carbon nanotube (CNT) nanocomposites. *Ceram. Int.* **40** (2014), 511-16.

[20] N. Doostdar, C. Smith, M. B. Hamill, A. R. Barron, Synthesis of calcium-silica composites: a route towards an in-vitro model system for calcific band keratopathy precipitates, *J. Biomed Mater. Res*., **99A** (2011), 173-183.

[21] A. J. Allen, J. J. Thomas, H. M. Jennings, Composition and density of nanoscale calcium–silicate–hydrate in cement, *Nat. Mater.* **6** (2007), 311-316.

[22] E. A. Whitsitt, A. R. Barron, Silica coated single walled nanotubes, *Nano Lett*. 3 (2003), 775-778.

[23] H. R. Jafry, E. A. Whitsitt, A. R. Barron, Silica coating of vapor grown carbon fibers, *J. Mater. Sci*. **42** (2007) 7381-7388.

[24] E. A. Whitsitt, A. R. Barron, Effect of surfactant on particle morphology for liquid phase deposition of submicron silica, *J. Colloid Interface Sci*. **287** (2005), 318-325.

[25] A. W. Orbaek, N. Aggarwal, A. R. Barron, The development of a 'process map' for the growth of carbon nanomaterials from ferrocene by injection CVD, *J. Mater. Chem., A.* **1** (2013), 14122-14132.

[26] V. Gomez, S. Irusta, W. W. Adams, R. H. Hauge, C. W. Dunnill, A. R. Barron, Enhanced carbon nanotubes purification by physic-chemical treatment with microwave and Cl_2, *RSC Adv*. **6** (2016), 11895-11902.

[27] S. Musić, N. Filipović-Vinceković, L. Sekovanić, Precipitation of amorphous SiO_2 particles and their properties, *Braz. J. Chem. Eng.* **28** (2011), 89-94.

[28] A. Radha, T. Z. Forbes, C. E. Killian, P. Gilbert, A. Navrotsky, Transformation and crystallization energetics of synthetic and biogenic amorphous calcium carbonate*, Proc. Natl. Acad. Sci.* **2010,** *107,* 16438-16443.

[29] O. Nilsen, H. Fjellvåg, A. Kjekshus, Growth of calcium carbonate by the atomic layer chemical vapour deposition technique*, Thin Solid Films* **450** (2004), 240-247.

[30] B. Xu, K. M. Poduska, Linking crystal structure with temperature-sensitive vibrational modes in calcium carbonate minerals *Phys. Chem. Chem. Phys.* **16** (2014), 17634-17639.

[31] G. Laudisio, F. Branda, Sol–gel synthesis and crystallisation of $3CaO{\cdot}2SiO_2$ glassy powders, *Thermochim. Acta* **370** (2001), 119-124.

[32] M. K. Singh, A. Agarwal, R. Gopal, R. K. Swarnkar, R. K. Kotnala, Dumbbell shaped nickel nanocrystals synthesized by a laser induced fragmentation method, *J. Mater. Chem*. **21** (2011), 11074-11079.

[33] G. S. Pappas, P. Liatsi, I. A. Kartsonakis, I. Danilidis, G. Kordas, Synthesis and characterization of new SiO_2-CaO hollow nanospheres by sol–gel method: bioactivity of the new system*, J. Non-Cryst. Solids* **354** (2008), 755-760.

[34] A. Mahajan, A. Kingon, A. Kukovecz, P. M. Vilarinho, Studies on the thermal decomposition of multiwall carbon nanotubes under different atmospheres, *Mater. Lett.* **90** (2013), 165-168.

[35] V. Gomez, C. W. Dunnill, A. R. Barron. A microwave cured flux for the adhesion of ceramic particles using silica coated carbon nanotubes, *Carbon* **93** (2015); 774-781

[36] F. S. Murakami, P. O. Rodrigues, C. M. Teixeira de Campos, M. A. S. Silva, Physicochemical study of $CaCO_3$ from egg shells, *Ciênc. Tecnol. Aliment.* **27** (2007), 658-662.

[37] V. S. Ramachandran, R. M. Paroli, J. J. Beaudoin, A. H. Delgado, *Handbook of thermal analysis of construction materials*. William Andrew Publishing: New York, 2002.

[38] Fluorescence quenching of single walled carbon nanotubes in SDBS surfactant suspension by metal ions: quenching efficiency as a function of metal and nanotube identity. J, J. Brege, C. Gallaway, and A. R. Barron, *J. Phys. Chem., C*, 2007, **111**, 17812-17820.

[39] X. Gong, J. Liu, S. Baskaran, R. D. Voise, J. S. Young, Surfactant-assisted processing of carbon nanotube/polymer composites*, Chem. Mater.* **12** (2000), 1049-1052.

[40] A. Eitan, K. Jiang, D. Dukes, R. Andrews, L. S. Schadler, Surface modification of multiwalled carbon nanotubes: toward the tailoring of the interface in polymer composites, *Chem. Mater.* **15** (2003), 3198-3201.

Table 1

Samples composition.

Sample	Commercial $CaSiO_3$ (mg)	$CaCO_3$ (mg)	Fumed SiO_2 (mg)	Silicic acid (mg)	1% SDS in water (mL)	MWCNT 1% SDS (mL)
1		200	20		2	
2		200	20			2
3		200		20	2	
4		200		20		2
5	200				2	
6	200					2

Legends for Figures

Fig. 1. SEM micrograph of the as purified CNTs used in the present study.

Fig. 2. SEM images of (a) sample **2** ($CaCO_3$/FS/SDS-MWCNT) after (a) one and (b) two weeks of curing and (c) sample **1 (**$CaCO_3$/FS/SDS) with (d) its corresponding EDX spectrum showing the presence of residual SDS.

Fig. 3. XRD patterns for (a) samples **1** and **2**, (b) samples **3** and **4**, and (c) sample **5** and **6** as prepared and after sintering at 1300 °C.

Fig. 4. FTIR spectra for (a) samples **1** and **2**, (b) samples **3** and **4**, and (c) sample **5** and **6** as prepared and after sintering at 1300 °C.

Fig. 5. SEM micrographs of (a and b) sample **3** ($CaCO_3$/SA/SDS) and (c and d) sample **4** ($CaCO_3$/SA/SDS-MWCNT).

Fig. 6. SEM images of (a) commercial CaO-SiO_2 after curing in 1% SDS solution for one week (sample **5**) and (b) after sintering at 1300 °C, and (c) commercial CaO-SiO_2 after being curing in 1% SDS-MWCNT solution for one week (sample **6**) and (d) after sintering at 1300 °C.

Fig. 7. Differential thermal-thermogravimetric analysis (DT/TGA) of commercial CaO-SiO_2 cured in the presence of SDS (a and c) and SDS-MWCNTs (b and d).

Fig. 1.

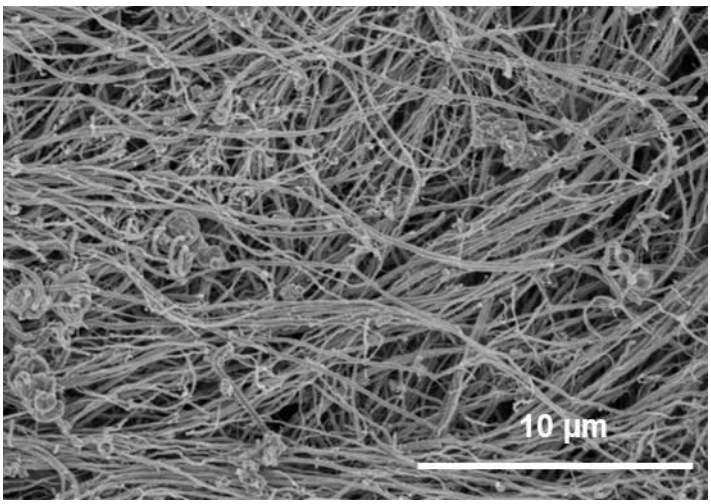

Fig. 2.

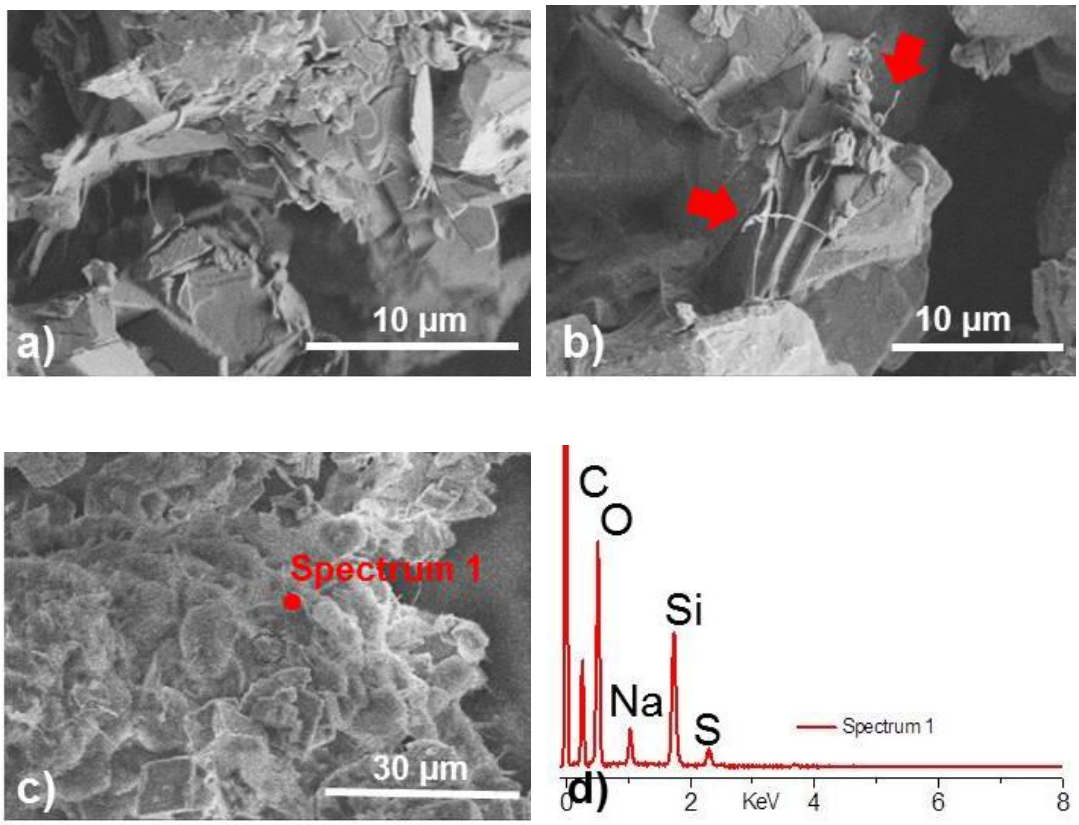

Fig. 3.

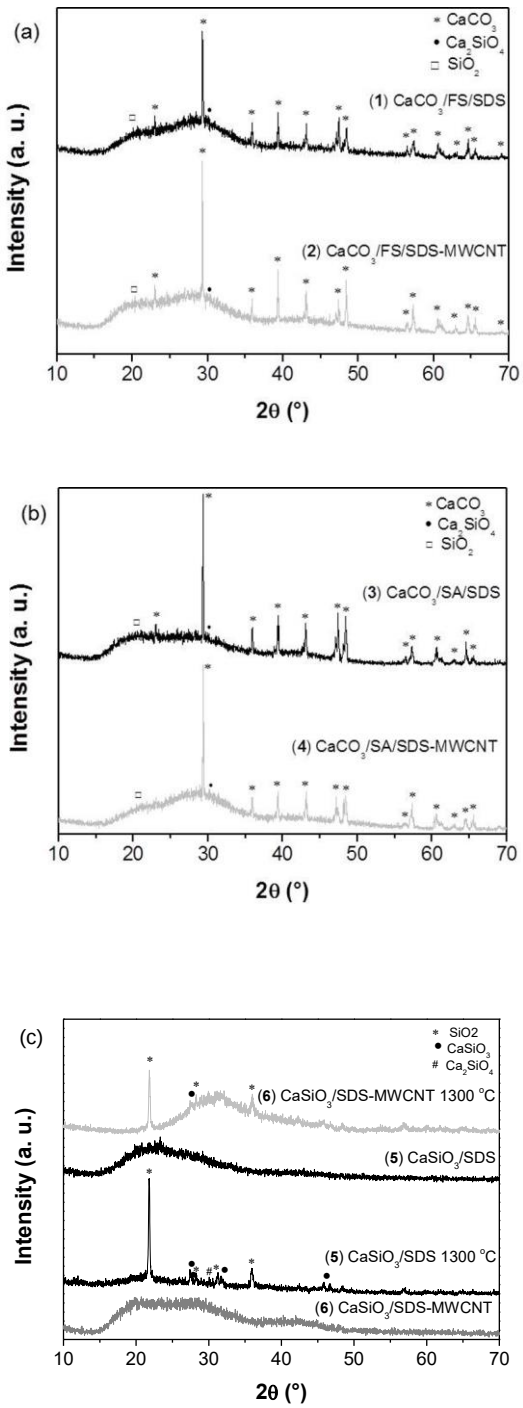
(a)
* CaCO3
• Ca2SiO4
□ SiO2
(1) CaCO3/FS/SDS
(2) CaCO3/FS/SDS-MWCNT
Intensity (a. u.)
2θ (°)
(b)
* CaCO3
• Ca2SiO4
□ SiO2
(3) CaCO3/SA/SDS
(4) CaCO3/SA/SDS-MWCNT
Intensity (a. u.)
2θ (°)
(c)
* SiO2
• CaSiO3
Ca2SiO4
(6) CaSiO3/SDS-MWCNT 1300 °C
(5) CaSiO3/SDS
(5) CaSiO3/SDS 1300 °C
(6) CaSiO3/SDS-MWCNT
Intensity (a. u.)
2θ (°)

Fig. 4.

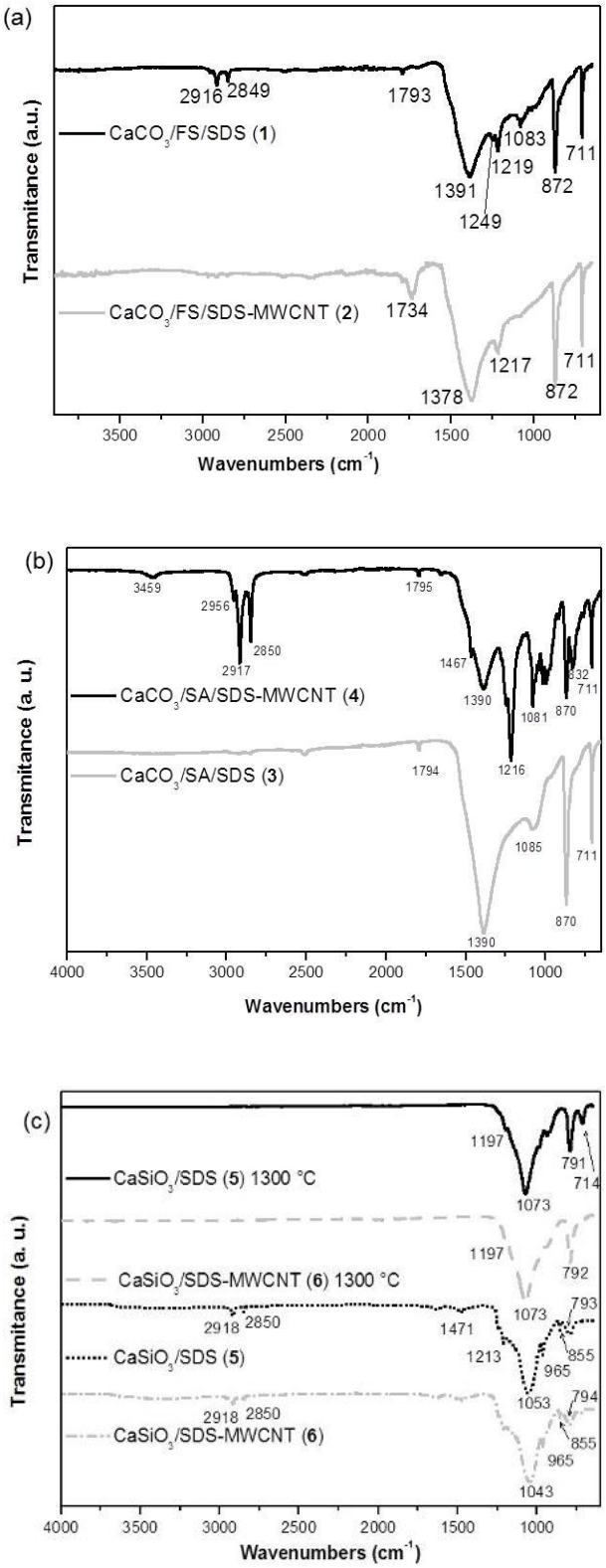
(a)
2916
2849
1793
CaCO3/FS/SDS (1)
1083
1219
711
872
1391
1249
CaCO3/FS/SDS-MWCNT (2)
1734
1217
711
872
1378
Transmitance (a.u.)
3500
3000
2500
2000
1500
1000
Wavenumbers (cm-1)
(b)
3459
2956
2917
2850
1795
1467
1390
1081
870
832
711
CaCO3/SA/SDS-MWCNT (4)
CaCO3/SA/SDS (3)
1794
1216
1085
711
870
1390
Transmitance (a. u.)
4000
3500
3000
2500
2000
1500
1000
Wavenumbers (cm-1)
(c)
1197
791
714
1073
CaSiO3/SDS (5) 1300 °C
1197
792
CaSiO3/SDS-MWCNT (6) 1300 °C
1073
793
2918
2850
1471
1213
855
965
CaSiO3/SDS (5)
1053
794
2918
2850
855
965
CaSiO3/SDS-MWCNT (6)
1043
Transmitance (a. u.)
4000
3500
3000
2500
2000
1500
1000
Wavenumbers (cm-1)

Fig. 5.

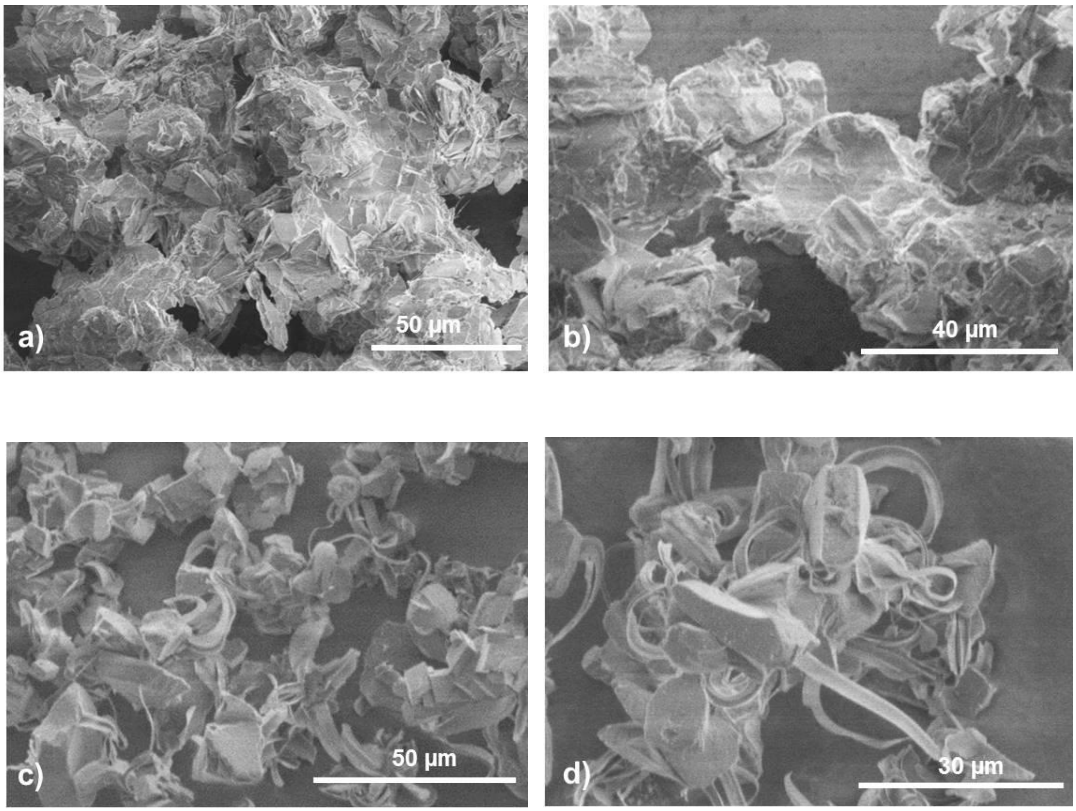

Fig. 6.

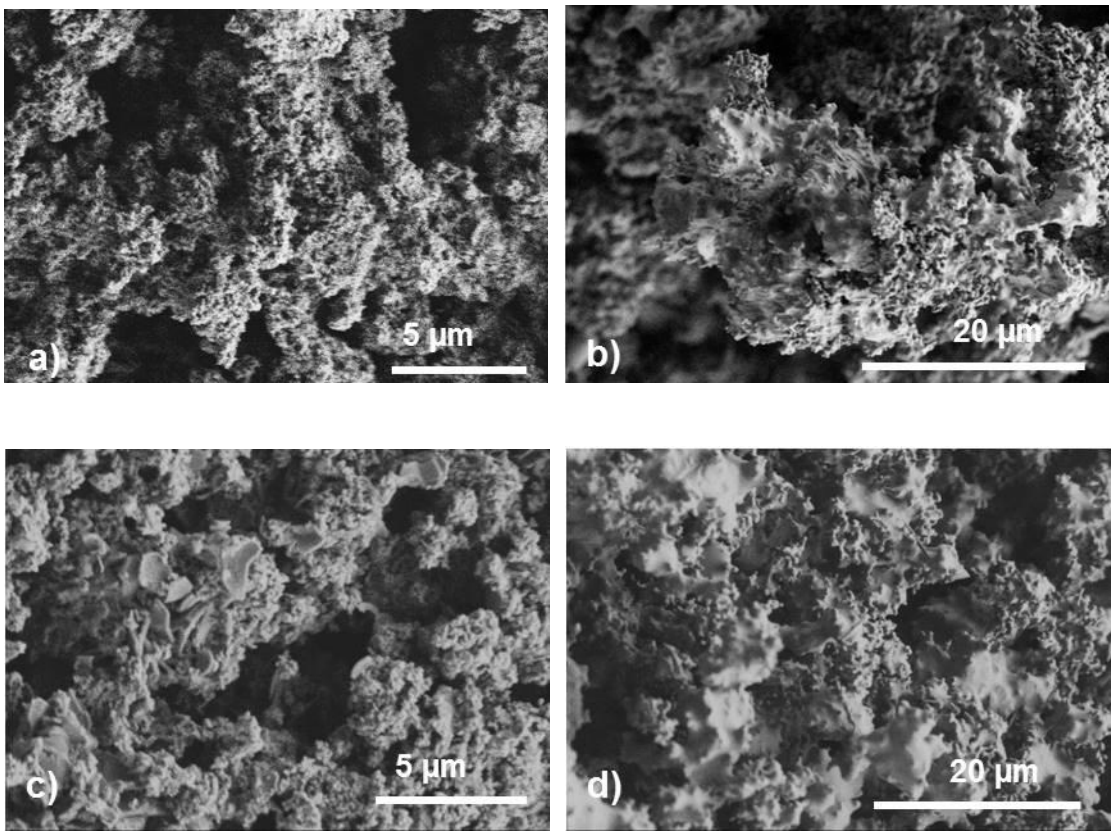

Fig. 7.

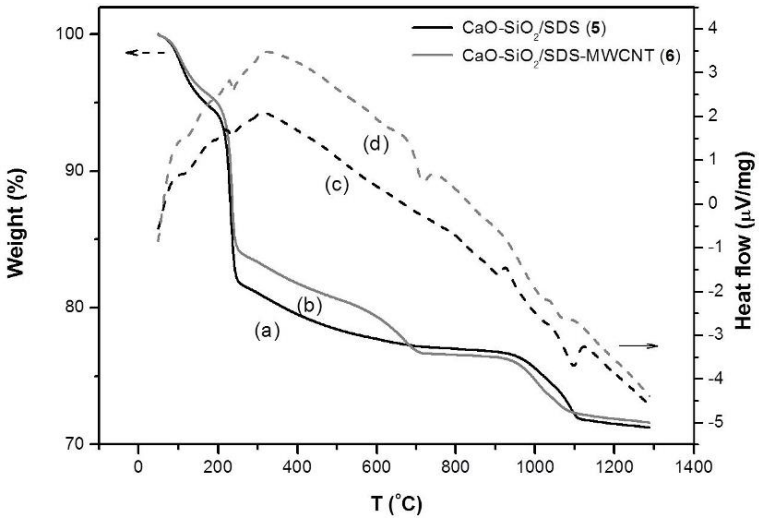
CaO-SiO2/SDS (5)
CaO-SiO2/SDS-MWCNT (6)
(a)
(b)
(c)
(d)
Weight (%)
Heat flow (μV/mg)
T (°C)
100
90
80
70
0
200
400
600
800
1000
1200
1400
4
3
2
1
0
-1
-2
-3
-4
-5